HAL open science

Enhancing peripheral scene recognition through spatial frequency training: Behavioral evidence from macular degeneration and healthy aging

Cynthia Faurite, Célia Michaud, Pauline Olivier, Mathilde Gallice, Christophe Chiquet, Vincent Soler, Isabelle Berry, Benoit R Cottereau, Carole Peyrin

To cite this version:

Cynthia Faurite, Célia Michaud, Pauline Olivier, Mathilde Gallice, Christophe Chiquet, et al.. Enhancing peripheral scene recognition through spatial frequency training: Behavioral evidence from macular degeneration and healthy aging. Neuropsychologia, 2026, 223, pp.109377. 10.1016/j.neuropsychologia.2026.109377 . hal-05506387

HAL Id: hal-05506387

https://hal.science/hal-05506387v1

Submitted on 12 Feb 2026

HAL is a multi-disciplinary open access archive for the deposit and dissemination of scientific research documents, whether they are published or not. The documents may come from teaching and research institutions in France or abroad, or from public or private research centers.

L'archive ouverte pluridisciplinaire **HAL**, est destinée au dépôt et à la diffusion de documents scientifiques de niveau recherche, publiés ou non, émanant des établissements d'enseignement et de recherche français ou étrangers, des laboratoires publics ou privés.

Distributed under a Creative Commons CC BY 4.0 - Attribution - International License

Author Accepted Manuscript (AAM)
Faurite, C., Michaud, C., Olivier, P., Gallice, M., Chiquet, C., Soler, V., Berry, I., Cottereau, B. R., & Peyrin, C. (2026). Enhancing peripheral scene recognition through spatial frequency training: Behavioral evidence from macular degeneration and healthy aging. Neuropsychologia.
https://doi.org/10.1016/j.neuropsychologia.2026.109377

This manuscript is made available under a CC BY 4.0 licence in accordance with the CNRS rights-retention strategy.
The final published version is available from Elsevier.

Enhancing peripheral scene recognition through spatial frequency training: Behavioral evidence from macular degeneration and healthy aging

Cynthia Faurite[1#], Célia Michaud[2#], Pauline Olivier[1], Mathilde Gallice[3], Christophe Chiquet[3], Vincent Soler[2], Isabelle Berry[2], Benoit R. Cottereau[2,4*], & Carole Peyrin[1*]

1. Univ. Grenoble Alpes, Univ. Savoie Mont Blanc, CNRS, LPNC, Grenoble, France
2. CerCo UMR 5549, CNRS – Université Toulouse III, Toulouse, France
3. Department of Ophthalmology, Grenoble Alpes University Hospital, Grenoble, France
4. IPAL, CNRS IRL 2955, Singapore.

# These authors contributed equally to this work.

* Co-senior authors.

Short title: Training scene recognition in macular degeneration and aging

***Corresponding Author:**

Carole Peyrin, PhD

Laboratoire de Psychologie et NeuroCognition (LPNC)

CNRS UMR 5105 - Université Grenoble Alpes

BMD - 1251 Av Centrale CS40700

38058 Grenoble Cedex 9 - France

carole.peyrin@univ-grenoble-alpes.fr

Abstract

Macular degeneration (MD) causes central vision loss and leads to long-term reorganization of visual functions. Central vision loss in MD severely reduces access to high spatial frequencies (HSF) that convey fine visual details, while low spatial frequencies (LSF) remain relatively accessible through peripheral vision and may support compensatory processing. This study investigated whether repeated training in categorizing filtered scenes improves peripheral scene recognition by enhancing spatial frequency processing. Ten MD patients and ten age- and gender-matched controls performed a scene categorization task (indoor vs. outdoor) using LSF or HSF images. Both groups completed a 12-session training protocol: patients performed the task at their preferred retinal location (PRL), and controls fixated with their fovea and viewed stimuli through an individualized artificial scotoma matched to their paired patient. Before training, MD patients showed a marked deficit for HSF scenes compared to controls, and a milder deficit for LSF scenes. After training, patients exhibited a significant improvement in categorizing LSF scenes, and an improvement specifically limited to HSF outdoor scenes, suggesting enhanced use of preserved peripheral information and partial compensation for the HSF deficit. Older controls also showed reduced performance for HSF scenes in peripheral vision, and similarly benefited from training. These results highlight the potential of perceptual training to enhance peripheral visual processing in MD patients, particularly by leveraging coarse visual cues. They support the idea that such protocols may be beneficial not only for visual rehabilitation in MD but also for preserving visual-cognitive functions in normal aging.

Keywords: Central vision loss; Peripheral vision; Spatial frequencies; Scene categorization; Visual training; Visual aging.

1. Introduction

Macular degeneration (MD) is a common retinal disorder characterized by progressive damage to the macula, the central part of the retina responsible for high-acuity vision (Mitchell & Bradley, 2006; Lim et al., 2012). It is among the leading causes of visual impairment in industrialized countries and results in central vision loss, particularly affecting tasks that rely on fine detail processing (Mitchell & Bradley, 2006). Age-related macular degeneration (AMD) is the most prevalent form of MD, accounting for the majority of cases. Worldwide, AMD was projected to affect approximately 288 million by 2040 (Wong et al., 2014). However, only a fraction of these individuals develop visual impairment. Recent GBD-based estimates indicate that AMD-related low vision and blindness affected about 8 million people in 2021, with projections suggesting a continued rise to around 14-21 million cases by 2050 (Zhang et al., 2024; GBD 2021 Global AMD Collaborators, 2025). AMD exists in two main forms: the atrophic (dry) form, which accounts for about 80-85% of cases, and the exudative (wet) form, characterized by abnormal blood vessel growth under the macula and affecting the remaining 15-20% of cases (Thomas et al., 2021). While several treatments have proven effective for the wet form, such as intravitreal injections of vascular endothelial growth factor (VEGF) inhibitors (Hussain & Ciulla, 2017; Solomon et al., 2019), laser photocoagulation (Shah & Shah, 2011), or photodynamic therapy (Awan & Tarin, 2006), no therapeutic intervention has yet been shown to slow or reverse the atrophic form. Similar mechanisms of central retinal degeneration are observed in Stargardt disease (STG), the most common form of juvenile macular dystrophy, which is caused by mutations in the ABCA4 gene (Allikmets et al., 1997). Like dry AMD, STG leads to progressive central vision loss and currently lacks any curative treatment. In the absence of effective therapies, visual rehabilitation strategies play a crucial role in helping patients adapt to visual impairment and preserve their quality of life.

Patients with AMD and STG typically suffer from dense central scotomas, corresponding to areas of absolute vision loss, as well as reduced sensitivity in the surrounding foveal region (Sunness et al., 1996), both of which severely compromise visual processing. This loss of central vision affects many daily activities that rely on high-level visual functions, such as reading (Legge et al., 1992; Fine et al., 1995; Fletcher et al., 1999), driving (Rovner & Casten, 2002), face recognition (Bullimore et al., 1991; Peli et al., 1994; Tejeria et al., 2002), understanding facial expressions (Boucart et al., 2008b), scene recognition (Boucart et al., 2008a), and mobility (Salive et al., 1994; Hassan et al., 2002). These limitations contribute to a decline in quality of life (Brown et al., 2002), often accompanied by social isolation and

depression (Brody et al., 2001; Rovner & Casten, 2002). Although some peripheral vision is usually preserved, it remains limited in its ability to compensate for the loss of foveal input. Many patients adopt a preferred retinal locus (PRL), a fixation point in the peripheral retina used to compensate for central vision loss (Crossland et al., 2011). However, this adaptation rarely restores normal visual function.

Peripheral vision alone is often insufficient to support tasks requiring high spatial frequency (HSF) processing, such as reading or face recognition (Logan et al., 2020; Calabrèse et al., 2011). However, low spatial frequencies (LSF) remain relatively preserved (Musel et al., 2011; Peyrin et al., 2017). This dissociation reflects the anatomical specialization of the visual system. The central retina is dominated by parvocellular pathways tuned to HSF, whereas the peripheral retina is primarily magnocellular and more sensitive to LSF (Curcio & Allen, 1990; Curcio et al., 1990; Wässle et al., 1990). Behavioral studies confirm that patients retain LSF-based categorization abilities but are markedly impaired when recognition relies on HSF (Musel et al., 2011; Peyrin et al., 2017; Ramanoël et al., 2018). These findings support the idea that residual peripheral vision can support certain perceptual functions, particularly the extraction of global scene structure.

Understanding which visual functions are preserved despite central lesions and how functional adaptations emerge is a key issue for both clinical research and practice, as it guides the development of appropriate rehabilitation strategies and supports patients' psychosocial adjustment (Mitchell & Bradley, 2006). In a recent study, Faurite et al. (2025) addressed these questions by comparing scene recognition performance in patients with MD and in age and gender matched sighted controls. All participants were tested monocularly, with the non-tested eye covered with a patch. This was essential because the characteristics of the visual deficit such as scotoma size, location of the PRL, and visual acuity often differ between the two eyes. Testing one eye at a time allowed for precise control over the retinal area used for fixation and stimulation. Participants performed a scene categorization task with images filtered in low or high spatial frequencies. Patients used their PRL to fixate, while controls were tested under matched visual constraints, maintaining fixation on the retinal location corresponding to their paired patient's fovea, within an artificial scotoma. This design allowed to compare groups under equivalent peripheral viewing conditions. Behavioral performance was measured during an fMRI session to assess both accuracy and associated brain activity. Patients exhibited significantly lower performance than controls for both types of stimuli, with a more pronounced deficit for high spatial frequencies. Functional MRI analyses revealed reduced activation in occipital areas and in the parahippocampal place area (PPA), particularly for high-

frequency scenes. In contrast, low-frequency processing was relatively preserved and associated with increased activity in higher-level cognitive and oculomotor regions. These findings show that macular disease alters spatial frequency processing even within the residual visual field and that partial compensation can emerge through functional reorganization. This dual pattern of degradation and adaptation highlights the need to better understand which functions can be supported by peripheral vision, and how to promote them effectively in rehabilitation.

In this context, several rehabilitation programs have been developed to help patients make better use of their residual vision. Most of them have focused on optimizing the use of the preferred retinal locus (PRL), typically through fixation tasks with real-time feedback to improve oculomotor control and reading performance (Culham et al., 1997; Rosengarth et al., 2013; Melillo et al., 2020). Such training can lead to improvements in visual acuity and reading speed, and sometimes in quality of life or mental health outcomes (Seiple et al., 2005; Sahli et al., 2020). In addition, microperimetric biofeedback training in AMD has been reported to enhance luminance contrast sensitivity more strongly at LSF than at HSF (Barboni et al., 2019), an effect interpreted by the authors as resulting from improved fixation stability and PRL positioning. Overall, these oculomotor-based interventions can indirectly facilitate access to residual visual information, but they do not directly train the spatial-frequency processing mechanisms that limit perceptual performance in peripheral vision.

To complement these oculomotor approaches, perceptual learning has emerged as a promising method to enhance residual visual functions. This technique involves repeated exposure to specific visual tasks and has been shown to induce long-lasting improvements in contrast sensitivity, visual acuity, and higher-level visual functions (Karni & Sagi, 1991; Casco et al., 2004; Chung, 2011; Maniglia et al., 2016; Sasso et al., 2019). Among the few studies targeting perceptual abilities in macular disease, Maniglia et al. (2018) applied a perceptual learning protocol based on lateral masking. Patients were trained to detect low-contrast Gabor patches flanked by high-contrast elements, presented at their PRL. The flankers were arranged in collinear or orthogonal configurations at varying distances to probe lateral interactions, which reflect the size and functional properties of perceptual fields. In healthy observers, the distance at which flankers shift from inhibiting to facilitating target detection varies with eccentricity, being shorter in central than in peripheral vision, consistent with the organization of receptive fields (Maniglia et al., 2011). Maniglia et al. (2011) found that some patients exhibited reduced collinear inhibition, a pattern typically associated with smaller, more fovea-like perceptual fields. After training, a further reduction in collinear inhibition was observed in

patients but not in controls, suggesting functional reorganization in cortical regions associated with the PRL.

While promising, these protocols typically rely on low-level visual stimuli and do not directly address higher-order visual functions. In this context, we sought to extend perceptual learning to more ecological and cognitively demanding tasks.

This study aimed to test whether training with spatially filtered real-world scenes could enhance scene categorization in peripheral vision, particularly in patients with MD. Unlike conventional perceptual learning paradigms using simple stimuli, we used complex, ecologically valid images to engage higher-level visual functions. To our knowledge, this is the first study to evaluate scene-based perceptual training using spatial frequency manipulation in peripheral vision, offering novel insights into both clinical rehabilitation and healthy aging. We hypothesized that patients with MD would show greater deficits for high spatial frequency scenes, and that training would help compensate for this impairment. To this end, we developed a training protocol using filtered real-world scenes to strengthen visual adaptations in patients with MD. Ten patients took part in the training, including the seven reported in the previous study (Faurite et al., 2025). Over 12 sessions spread across four weeks, they categorized scenes filtered in either LSF or HSF while maintaining fixation with their PRL. The same task was used before and after training evaluations to assess improvements in performance. However, the images used during training differed from those used in the evaluations, ensuring that gains were not due to stimulus repetition. To assess whether the observed effects were specific to MD or could also occur in the context of normal aging, we included a group of age- and gender-matched healthy controls. Each patient was paired with a control participant who performed the same training under equivalent peripheral viewing constraints. Specifically, each control was instructed to maintain fixation on the retinal location corresponding to their matched patient's PRL, and viewed the scenes through an artificial central scotoma replicating the exact size and position of the patient's visual field loss. This individualized design allowed for a direct comparison under strictly matched peripheral vision conditions and helped isolate the impact of the pathology from age-related changes.

2. Method

2.1. Participants

Ten patients with MD and ten age- and gender-matched normally sighted controls were included in the study (Table 1). Patients were recruited from the Ophthalmology Department at Grenoble University Hospital (CHUGA) and the Retina Center at Purpan Hospital in

Toulouse. Seven of them were diagnosed with atrophic age-related macular degeneration (AMD) and three with a late form of Stargardt disease (STG). All patients had a confirmed diagnosis of macular disease characterized by bilateral central atrophy on multimodal imaging (fundus autofluorescence and spectral domain-optical coherence tomography, SD-OCT) and demonstrated a stable preferred retinal locus in at least one eye. Comprehensive ophthalmological screening ruled out additional ocular or neurological conditions that could affect peripheral vision or the visual pathways, including glaucoma, ocular hypertension, peripheral retinal dystrophies or degenerations, diabetic or hypertensive retinopathy with peripheral involvement, optic neuropathies, significant media opacities (corneal and lens diseases), or neurological disorders. All patients had bilateral central scotomas, with foveal sparing observed in patients MD2, MD5, and MD6. Each patient was matched with a control participant of the same gender, with an age difference of less than two years, except for MD2 (81 years) and the respective control C2 (75 years). One younger patient with STG (MD10, aged 25) with early-onset macular disease was also included in the sample. Given the strong age difference with the rest of the group, this participant and their matched control were taken into account in additional sensitivity analyses described in the Results section.

None of the participants reported chronic general medical conditions. Cognitive and psychological status were assessed using the Mini-Mental State Examination (MMSE) and the Beck Depression Inventory-II (BDI-II). All participants scored above 23 on the MMSE and below 19 on the BDI-II, indicating the absence of cognitive impairment or clinical depression. All participants provided written informed consent prior to inclusion. The study was approved by the French ethics committee (Comité de Protection des Personnes Sud Méditerranée IV, 2022-00957-36).

Table 1. Demographic and clinical characteristics of MD patients and their matched controls. The table includes the patient's code, gender, age and diagnosis (AMD or STG). Visual acuity for the left eye and right eye is reported in logMAR. Scotoma size is given as the radius in degrees. *For MD5, scotoma radius provides two values because this patient's scotoma was elliptical. Preferred fixation values are provided in polar angle (θ) and eccentricity (ρ) in degrees, as well as in degrees along the x- and y-radius. Foveal sparing is indicated as "Yes" if the preferred fixation position is within the first 1° of visual eccentricity. Each patient is numerically paired with a control subject matched for age and gender. Visual acuity was assessed using the Freiburg Visual Acuity Test (FrACT; Bach, 2007). Values corresponding to the tested eye are shown in bold.

Patients		**MD1**	**MD2**	**MD3**	**MD4**	**MD5**	**MD6**	**MD7**	**MD8**	**MD9**	**MD10**
Gender (F: Female | M: Male)		F	M	F	M	M	F	M	M	F	M
Age (years)		75	81	66	73	75	50	69	74	73	25
Diagnosis		AMD	AMD	AMD	AMD	AMD	STG	STG	AMD	AMD	STG
Visual acuity Before training (LogMar)	Left eye	**+0.8**	+1.5	**+0.2**	**+0.7**	+1.3	**+0.2**	+0.6	**+1.0**	+0.9	+0.4
	Right eye	+0.8	**+0.3**	+0.6	+0.7	**+0.6**	+0.2	**+0.6**	+1.2	**+0.3**	**+0.2**
Visual acuity After training (LogMar)	Left eye	**+0.9**	+1.5	**+0.3**	**+0.6**	+1.0	**+0.3**	+0.7	**+0.9**	+0.2	+0.4
	Right eye	+0.9	**+0.3**	+0.8	+0.4	**+0.6**	+0.2	**+0.6**	+0.9	**+0.1**	**+0.2**
Tested eye (L: Left | R: Right)		L	R	L	L	R	L	R	L	R	R
Atrophy area (mm²)		23.08	7.29	13.95	25.44	24.72	7.99	9.09	21.12	0.1	1.82
Scotoma radius (deg)		9.72	5.3	7.31	9.84	6.15 12.31*	5.18	5.87	8.25	0.62	2.64
Preferred fixation polar angle θ (deg)		152.64	-36.11	-22.7	180	28.47	0	90	-170.64	-90	-84.24
Preferred fixation eccentricity ρ (deg)		10.36	1.05	2.12	9.58	0.94	0	5.22	8.8	2.9	6.77
Preferred fixation coordinates (μm)	X axis	3239	-245	-565	2761	239	0	0	-2499	0	195
	Y axis	-1370	179	236	0	130	0	-1503	-410	-847	-1940
Preferred fixation coordinates (deg)	X axis	9.2	-0.85	-1.96	9.58	0.83	0.0	0.0	-8.68	0.0	0.68
	Y axis	-4.76	0.62	0.82	0.0	0.45	0.0	-5.22	-1.43	-2.9	-6.74
Foveal sparing		No	Yes	No	No	Yes	Yes	No	No	No	No
Matched controls		**C1**	**C2**	**C3**	**C4**	**C5**	**C6**	**C7**	**C8**	**C9**	**C10**
Gender (F: Female | M: Male)		F	M	F	M	M	F	M	M	F	M
Age (years)		74	75	67	71	77	52	68	76	70	26
Visual Acuity Before training (LogMAR)	Left eye	**-**0.2	0.0	**0.0**	**-0.1**	0.0	**-0.1**	0.0	**-0.2**	-0.2	-0.3
	Right eye	**-0.3**	**0.0**	+0.2	-0.2	**-0.2**	0.0	**-0.3**	0.2	**-0.1**	**-0.3**
Visual Acuity After training (LogMAR)	Left eye	**-**0.1	-0.2	**-0.1**	**0.0**	+0.1	**-0.1**	-0.1	**-0.2**	0.0	-0.3
	Right eye	**-0.2**	**-0.2**	+0.3	-0.2	**-0.2**	0.0	**-0.3**	-0.1	**0.0**	**-0.3**
Tested eye (L: Left | R: Right)		R	R	L	L	R	L	R	L	R	R

2.2. Visual Assessment and Scotoma Characterization

Patients first underwent monocular visual acuity assessment using the ETDRS (Early Treatment Diabetic Retinopathy Study) scale, as part of a comprehensive ophthalmological

examination that included refraction assessment and updating of optical correction when necessary. Visual acuity was assessed in order to confirm that patients met the inclusion criterion of having a monocular acuity better than 20/400 in the trained eye. Visual acuity was measured under the patients' habitual optical correction. Scotoma contours were delineated from autofluorescence fundus images by an ophthalmologist, who also calculated their surface area (in mm^2) for each eye (see Figure 1 and Table 1). Scotoma radius (in degrees of visual angle) was then estimated, assuming that 288 µm on the image corresponds to 1° of visual angle. For patient MD5, whose scotoma was elliptical, width was also measured along both vertical and horizontal axes.

OCT (Optical Coherence Tomography) was used to identify the preferred retinal locus (PRL) for each eye and to determine its retinal coordinates relative to the anatomical fovea (Table 1). During this examination, patients were instructed to fixate the OCT internal luminous target while three short fixation recordings were acquired for each eye. PRL stability was assessed from these repeated acquisitions, and a PRL was classified as stable when patients consistently used the same eccentric fixation region across recordings without a systematic shift to another retinal area. MD1 had developed a stable PRL only in the left eye, which was selected for testing. Despite presenting a central scotoma, MD6 showed foveal sparing and maintained foveal fixation in both eyes, a phenomenon frequently observed in late-stage STG (van Huet et al., 2014). Five patients fixated near the fovea in both eyes. The other seven patients had developed a stable PRL at the border of the scotoma in each eye.

For MD2, MD3, MD5, MD8, MD9, and MD10, the tested eye was chosen based on the best visual acuity (better than 20/400), following common practices in low-vision research, particularly when studying compensation mechanisms. Previous studies have shown that the PRL tends to be more stable and better optimized in the eye with higher acuity (Tarita-Nistor et al., 2023). For MD4, MD6, and MD7, whose acuity was similar in both eyes, the choice of tested eye was left to the participant.

Artificial scotomas were then constructed for each control participant based on the shape, radius, and surface area of the tested eye of their matched patient (Figure 1; see also Guénot et al., 2022, and Michaud et al., 2025). These artificial scotomas were circular, except for the one derived from MD5, which had an elliptical shape. Scotoma size and PRL location were used to align each artificial scotoma within the control participant's visual field, relative to the matched patient's PRL, and to constrain fixation accordingly during the experiment (see Procedure). In this study, the anatomical extent of retinal atrophy derived from fundus autofluorescence and OCT was therefore used as a pragmatic proxy for the spatial extent of

vision loss when defining artificial scotomas in controls. We acknowledge that anatomical and functional scotoma boundaries do not necessarily coincide, particularly in cases of partial foveal sparing or PRLs located close to the scotoma border. Systematic functional mapping of the scotoma with microperimetry would provide a more direct characterization of sensitivity loss, but such measures were not available for all patients and could not be integrated homogeneously across participants. The use of anatomical measures nevertheless allowed standardized, individualized matching between patients and controls and the imposition of comparable peripheral viewing constraints in both groups.

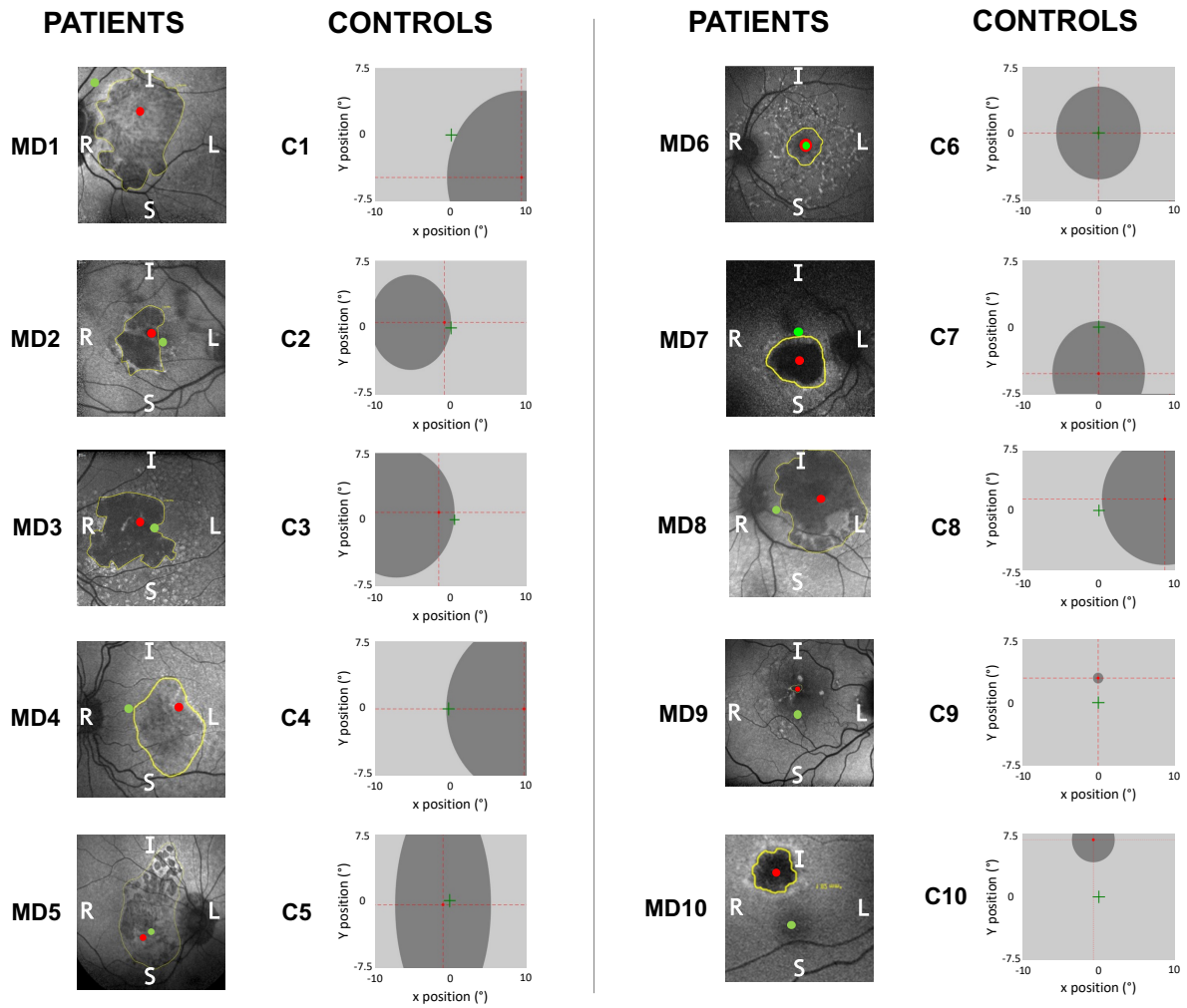

Figure 1. For each MD patient, autofluorescence images are displayed following the radiological convention: the anatomical left side of the retina (L) appears on the right of the image, and the anatomical right side (R) appears on the left. The images were then horizontally flipped to match the visual field orientation: the inferior (I) retina is shown at the top and the superior (S) retina at the bottom. The foveal position is indicated by a red dot, and the preferred fixation point by a green dot. For each matched control, the figure depicts the scotoma representation together with the positions of the fovea and fixation on a screen with the same dimensions as the stimuli used in both experiments (20° × 15° of visual angle). This depiction accounts for the optical inversion of the retinal image: the right visual field is shown on the right, the left visual field on the left, the upper visual field at the top, and the lower visual field at the bottom.

Control participants used their habitual, up-to-date optical correction and had normal or corrected-to-normal visual acuity (better than 0.1 LogMAR in the tested eye) and no history of ocular pathology. Visual acuity was measured before and after training using the Sloan letters of the Freiburg Visual Acuity Test (FrACT; Bach, 2007).

2.3. Stimuli and Procedure

The stimuli set was based on 80 photographs of real-world scenes (40 indoor and 40 outdoor scenes). Twenty of these scenes were used before and after training assessments. The remaining 60 images were used during the 12 training sessions and divided into three lists of 20 images each. Stimuli were created in MATLAB 2020b (MathWorks Inc., Sherborn, MA). Monitor gamma was estimated using a calibration device (Spyder5ELITE, Datacolor), and images were inverse-gamma corrected during stimulus construction to linearize luminance. All spatial filtering and contrast normalization were performed in linear luminance space.

Each image (see Figure 2) was filtered to create low spatial frequency (LSF) stimuli using three low-pass filters with cutoff frequencies set at 1, 1.4, and 2 cycles per degree (cpd, corresponding to 20, 28, and 40 cycles per image), and high spatial frequency (HSF) stimuli using three high-pass filters with cutoff frequencies set at 2.9, 4.6, and 6 cpd (corresponding to 58, 64, and 120 cycles per image). The frequency content of the scenes was filtered by multiplying the Fourier-transformed images by Gaussian filters. The standard deviation of each filter, defined by its cutoff frequency, ensured a standard 3 dB attenuation. The cutoff frequency was varied to modulate task difficulty.

We then normalized the luminance contrast of all LSF and HSF stimuli to a mean luminance of 128 on a 256-level grayscale scale, and to a root mean square (RMS) contrast of 0.1 (i.e., 25.6 on a 256-level grayscale scale). RMS normalization increased the contrast of HSF images while reducing that of LSF images. This manipulation was intended to eliminate any contrast bias, to prevent patients from experiencing excessive difficulty in categorizing HSF-filtered scenes (Peyrin et al., 2017), and to avoid ceiling effects in the categorization of LSF scenes. To preserve filtering conditions, the stimuli were resized to subtend a visual angle of 20° × 15° (i.e., 873 × 640 pixels), and were viewed at a distance of 55 cm. Because of potential left-right asymmetries in scene content and the risk of parts being masked by the scotoma, each stimulus was presented in both its original and mirrored configurations. All stimuli used in this study are available on the Open Science Framework (OSF) repository: https://osf.io/7hksz/.

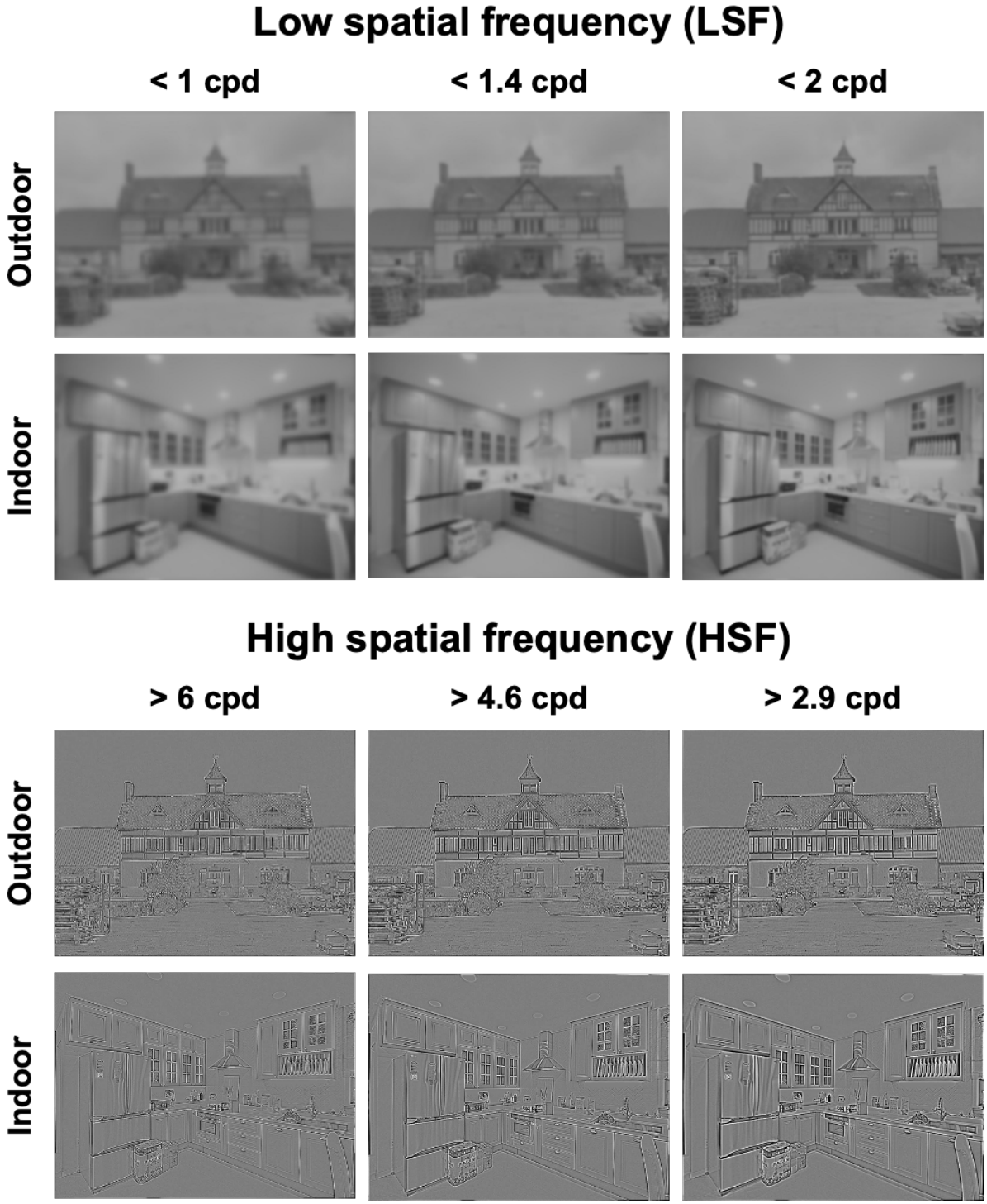

Figure 2. Examples of low spatial frequency (LSF) and high spatial frequency (HSF) scene stimuli from the indoor and outdoor categories. Stimuli were filtered using multiple cutoff frequencies: LSF images with low-pass filters at 1, 1.4, and 2 cycles per degree (20, 28, and 40 cycles per image), and HSF images with high-pass filters at 2.9, 4.6, and 6 cycles per degree (58, 64, and 120 cycles per image). Note that the perceived spatial frequency content may be affected by image downscaling for illustrative purposes.

Stimuli were presented using Psychtoolbox (Brainard, 1997; Kleiner et al., 2007) integrated with MATLAB 2020b (MathWorks Inc., Sherborn, MA). The room was consistently kept dimly lit, and the monitor served as the main source of illumination during stimulus presentation, ensuring a stable light-adaptation state across sessions and participants. Ambient illumination was therefore maintained at a constant level that did not vary across visits. The same scene categorization task was used before, during, and after training sessions. However, different sets of images were used during training and testing to avoid repetition effects. Participants completed 14 sessions in total, in the following order: one before training evaluation session, twelve training sessions over four weeks, and one after training evaluation session. Participants completed twelve training sessions over four weeks, corresponding to approximately three sessions per week. Sessions were scheduled according to participant availability, with at least 24 hours between consecutive sessions and no more than one session completed per day. Because training effects were evaluated within each participant relative to their own baseline performance, variability in testing time does not prevent assessing whether performance improved over the course of training.

Both patients and controls followed this exact same protocol. The stimuli used before and after training assessments were strictly identical. During the training sessions, a different set of scenes was used, distributed across three counterbalanced image lists. LSF and HSF stimuli were presented in alternating blocks. In each session, participants completed 10 alternating LSF/HSF blocks of 12 trials each (6 indoor and 6 outdoor scenes), totaling 240 trials per session. Each session lasted approximately 15 minutes. Stimulus presentation, fixation instructions, and task demands were identical across sessions. Each scene was displayed for 150 ms on a gray background, followed by a 2000 ms gray interstimulus interval. Participants were instructed to categorize each scene as either indoor or outdoor using response buttons. Errors and response times were recorded.

A red fixation cross (1° visual angle) remained on screen throughout the session to guide participants' gaze, with fixation instructions differing between patients and controls. All participants viewed the display with the tested eye, while the other eye was covered with an eye patch. Patients were instructed to fixate the red cross, placed at the center of the scenes, using their PRL and to maintain stable fixation. Control participants were tested with the same eye as their matched patient, except for C1, who used the other eye because preliminary task testing indicated better performance with that eye. No clinical or technical reason was identified to explain this difference. Controls were asked to fixate the red cross with their fovea, positioned at the same distance from the PRL as in the matched patient, to project visual

information onto comparable retinal regions across groups. In controls, an artificial scotoma was overlaid on the scenes, replicating the size and location of the matched patient's visual field loss based on the anatomical extent of retinal atrophy and PRL location (Figure 1). The parameters of this artificial scotoma were derived from the anatomical estimates described in the Visual Assessment and Scotoma Characterization section. The scotoma was black and circular in most cases, except for C5, who was shown an elliptical mask replicating MD5's scotoma more accurately. The artificial scotoma was centered on the fovea, except for C2 and C3, where it was laterally shifted to account for the asymmetrical extent of MD2 and MD3's scotomas, which extended further into the left visual hemifield.

2.4. Additional evaluations

Before and after training, we measured visual acuity using the Sloan letters from the Freiburg Visual Acuity Test (FrACT; Bach, 2007) for all participants. This test provided a logMAR (logarithm of the minimum angle of resolution) measure of visual acuity for each participant. We also assessed patients' mental health using the Beck Depression Inventory-II (BDI-II; Beck et al., 1996). This self-report questionnaire includes 21 items, each describing a symptom of depression. Each item is rated on a 0-to-3 scale, with higher scores indicating greater symptom severity. The sum of all items yields a total score ranging from 0 to 63. In accordance with our exclusion criteria, the maximum allowed score was 19. Finally, we evaluated vision-related quality of life using the National Eye Institute Visual Function Questionnaire (NEI-VFQ 25; Mangione et al., 1998). This 25-item questionnaire covers multiple dimensions of vision-related quality of life, including general health, general vision, ocular pain, near and distance activities, social functioning, mental health, role difficulties, dependency, driving, color vision, and peripheral vision. Each item is scored on a 1-to-5 scale. Scores were then converted to a 0-to-100 scale using a standardized conversion table. Higher scores indicate better perceived quality of life in the corresponding domain. For example, a score of 50 reflects 50% of the maximum possible score. Each domain aggregates several items, and a mean score was computed for each domain to provide a global score.

2.5. Data Analyses

Statistical analyses were conducted using R (R Core Team, 2021) and the *lme4* package (Bates, Mächler, et al., 2015). We built two models: one to analyze spatial frequency processing before training and another to assess the effect of training. To analyze the effects of spatial frequency cut-offs, we built separate models for LSF and HSF. Therefore, four models

were constructed: two to assess the spatial frequency cut-offs before training (one for LSF and one for HSF) and two to assess the effect of training (one for LSF and one for HSF). Due to the high error rates observed in patients, the number of valid reaction times was insufficient to perform reliable analyses on response latencies.

In all models, we analyzed trial-level categorization errors using generalized linear mixed-effects models (GLMMs) with a binomial error distribution. Incorrect responses were coded as 1 and correct responses as 0. GLMMs use each trial as a data point and estimate population-level effects (fixed effects) while modeling variability associated with participants and stimuli as random effects. This multi-level structure accommodates interindividual and item-related variability within the model itself and reduces the need to introduce separate covariates for each potential source of variation. GLMMs are well suited for binary outcome data, such as correct versus incorrect responses, because they estimate how performance changes across conditions while accounting for random variability across participants and items. Since analyses are performed on binary trial outcomes rather than aggregated percentages, this approach remains appropriate when performance approaches floor or ceiling levels in some conditions and avoids distortions associated with bounded data (see also Šimkovic & Träuble, 2019). The model examining spatial frequency processing before training included fixed effects for group (patients, controls), spatial frequency (LSF, HSF), and scene category (indoor, outdoor). The training effect model included fixed effects for group, spatial frequency, scene category, and training (before, after). The model examining pre-training LSF cut-offs included fixed effects of group (patients, controls), scene category (indoor, outdoor), and LSF cut-offs (1, 1.4, 2 cpd). The model assessing the training effect for LSF cut-offs included fixed effects of group (patients, controls), scene category (indoor, outdoor), LSF cut-offs (1, 1.4 and 2 cpd), and training (before, after). Similarly, the model examining pre-training HSF cut-offs included fixed effects of group (patients, controls), scene category (indoor, outdoor), and HSF cut-offs (2.9, 4.6, 6 cpd). The model assessing the training effect for HSF cut-offs included fixed effects of group (patients, controls), scene category (indoor, outdoor), HSF cut-offs (2.9, 4.6, 6 cpd), and training (before, after). In all models, participants, scotoma radius (x and y axes), distance between preferred fixation and the fovea (x and y axes), and stimuli were included as random effects. We specified random intercepts for participants, as well as random slopes for spatial frequency, scene category, training, spatial frequency cut-offs, and their interactions. The same random structure was used for the scotoma radius, fixation–fovea distances, and stimuli. To ensure model stability and avoid convergence issues, we followed the parsimonious modeling approach recommended by Bates, Kliegl, et al. (2015).

The significance threshold was set at $p < .05$. Post-hoc p-values were Bonferroni-corrected (multiplying each observed p-value by the number of comparisons, ranging from 2 to 4 depending on the analysis), using a conservative approach to reduce Type I error risk due to multiple testing.

We also evaluated the effect of training on other clinical and functional measures: visual acuity, quality of life, and mental health. We compared before and after training scores using appropriate statistical tests. As a reminder, visual acuity was measured with the FrACT test (Bach, 2007), vision-related quality of life with the NEI-VFQ 25 questionnaire (Mangione et al., 1998), and mental health with the BDI-II depression scale (Beck et al., 1996). For each measure, we used paired Wilcoxon tests (non-parametric), given the small sample size and sometimes non-normal distributions. Analyses were performed both on the global score and on the subscale scores of the NEI-VFQ 25. For visual acuity, the Wilcoxon test was applied to the score of the trained eye. The significance threshold was set at $p < .05$, with Bonferroni correction when multiple comparisons were conducted.

2.6. Hypotheses

Based on previous findings (Musel et al., 2011; Peyrin et al., 2017; Ramanoël et al., 2018; Faurite et al., 2025), we anticipated that, before training, patients with macular degeneration (MD) would show higher error rates than age-matched controls, especially for HSF scenes. This would result in an interaction between group and spatial frequency. We also expected that this deficit might vary depending on the scene category, as previously suggested (Musel et al., 2011; Faurite et al., 2025), indicating a potential three-way interaction between group, spatial frequency, and scene category.

We then formulated hypotheses regarding the effects of training on scene categorization performance. We expected an overall improvement in performance following training, particularly in the patient group, reflected in a group × training interaction. Given the more pronounced deficit in HSF processing in patients, we anticipated a group × training × spatial frequency interaction. Finally, we examined whether the scene category modulated the effect of training. To do so, we tested a four-way interaction (group × training × spatial frequency × category) to determine whether training yielded greater benefits for specific scene categories depending on their spatial frequency content.

3. Results

3.1. Spatial frequency processing before training

Statistical analyses revealed a significant main effect of the group, $\beta = -3.57$, $z = -8.4$, $p < .001$. Patients (mean ± standard error: 21.58 ± 0.2%) made more categorization errors than control participants (7.17 ± 0.13%). A significant main effect of spatial frequency was also observed, $\beta = -1.56$, $z = -2.43$, $p = .01$. Participants (both groups) made more errors for HSF scenes (19.27 ± 0.19%) than for LSF scenes (9.46 ± 0.15%). No significant interaction was found between group and spatial frequency, $\beta = 1.28$, $z = 1.54$, $p = .13$, nor between group, spatial frequency, and scene category, $\beta = -1.17$, $z = -0.88$, $p = .38$. These results may be influenced by the inclusion of one younger patient (MD10, aged 25, while other patients were aged 50–81), who showed a particularly low error rate (Figure 3; 3.69% vs. 22.73% on average for the other patients). We also ran a sensitivity analysis on a reduced sample of 9 patients and 9 matched controls over the age of 50, excluding MD10 and their matched control.

The new analyses confirmed a significant main effect of group, $\beta = -2.45$, $z = -3.45$, $p < .001$. Patients (23.65 ± 0.22%) made more errors than control participants (7.73 ± 0.14%). A significant main effect of spatial frequency was also found, $\beta = -2.21$, $z = -3.41$, $p < .001$. Both groups made more errors for HSF scenes (21.19 ± 0.21%) than for LSF scenes (10.19 ± 0.15%). This time, a significant interaction was found between group and spatial frequency, $\beta = 1.46$, $z = 2.93$, $p = .004$. Post-hoc comparisons showed that patients made significantly more errors for HSF scenes (29.32 ± 0.31%) than for LSF scenes (13.85 ± 0.24%), $\beta = 2.36$, $z = 3.32$, $p = .001$, while this difference was not significant for controls (HSF: 9.25 ± 0.20%; LSF: 5.08 ± 0.15%), $\beta = 1.2$, $z = 1.58$, $p = .12$. Patients made significantly more errors than controls only for HSF scenes, $\beta = 1.54$, $z = 2.98$, $p = .01$; for LSF scenes, the group difference did not reach significance, $\beta = 0.93$, $z = 2.01$, $p = .14$. No significant three-way interaction was found between group, spatial frequency, and semantic category, $\beta = -1.09$, $z = 1.63$, $p = .10$. Thus, we again observed a categorization deficit in MD patients, which was more pronounced for HSF than for LSF scenes, regardless of semantic category.

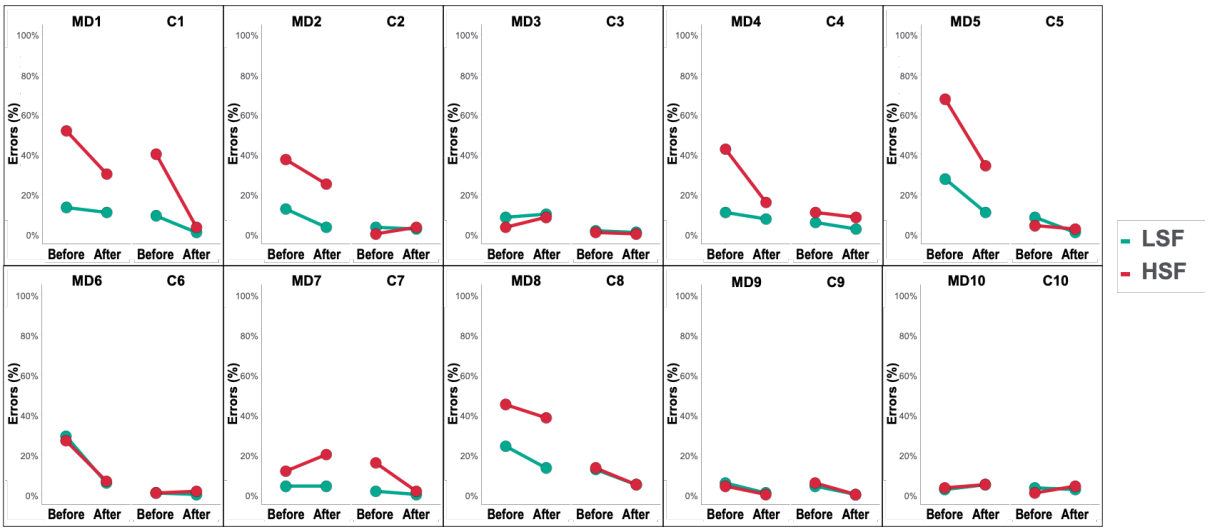

Figure 3. Error in percentage (%) for each patient (MD) and their matched control (C) when categorizing LSF (green) and HSF (red) scenes. Lines connect before and after training performances.

We also examined whether spatial frequency cut-off influenced pre-training categorization performance.

For LSF scenes, we observed a main effect of the spatial frequency cut-off, $\beta = -2.43$, $z = -2.01$, $p = .04$. Post-hoc comparisons revealed that participants (both patients and controls) made more errors at 1 cpd (11.39 ± 0.27%) than at 2 cpd (7.93 ± 0.23%), $\beta = -1.92$, $z = -1.97$, $p = .04$. However, the difference between 1 cpd and 1.4 cpd (11.25 ± 0.27%) was not significant, $\beta = -0.4$, $z = -0.47$, $p = .64$, nor was the difference between 1.4 cpd and 2 cpd, $\beta = -1.47$, $z = -1.64$, $p = .1$. There was no significant interaction between spatial frequency cut-off and the group, $\beta = -0.01$, $z = -0.01$, $p = .99$, or between group, spatial frequency cut-off, and scene category, $\beta = -1.02$, $z = -0.63$, $p = .53$.

For HSF scenes, we observed a significant main effect of spatial frequency cut-off, $\beta = -2.66$, $z = -3.49$, $p < .001$. Post-hoc comparisons revealed that participants (both patients and controls) made more errors at 6 cpd (28.09 ± 0.38%) than at both 4.6 cpd (20.47 ± 0.35%), $\beta = -1.41$, $z = -2.23$, $p = .03$, and 2.9 cpd (15 ± 0.31%), $\beta = -2.07$, $z = -2.85$, $p = .004$. However, the difference between 2.9 cpd and 4.6 cpd was not significant, $\beta = -0.52$, $z = -0.75$, $p = .46$. We also observed a significant interaction effect between spatial frequency cut-off and group, $\beta = -0.34$, $z = -3.18$, $p = .001$. Post-hoc comparisons showed that patients made significantly more errors than control participants at all HSF cutoffs tested, namely at 6 cpd (Patients: 41.5 ± 0.6%; Controls: 14.72 ± 0.43%, $\beta = -3.03$, $z = -2.39$, $p = .02$), at 4.6 cpd (Patients: 30.45 ± 0.56%; Controls: 10.56 ± 0.37%, $\beta = -2.98$, $z = -2.49$, $p = .01$) and at 2.9 cpd (Patients: 24.72

± 0.52%; Controls: 5.28 ± 0.27%, $\beta = -2.46$, $z = -2.85$, $p = .004$). The spatial frequency cut-off did not interact with group, and scene category, $\beta = 0.99$, $z = 0.71$, $p = .48$.

3.2. Training effects

Given the atypical performance of the younger patient (MD10), we tested training effects on the 9 patients aged over 50 (Figure 4). We compared performance between before and after training evaluation sessions. We did not statistically analyze performance across the 12 training sessions because three different scene lists were used and the list changed every four sessions. This design introduces variability linked to stimulus content rather than learning alone, which prevents a reliable evaluation of within-training progression. For this reason, Figure 5 is provided only as a descriptive illustration of session-by-session performance, while statistical analyses focus on identical pre- and post-training evaluation sessions.

3.2.1. Scene categorization performance

Analyses revealed a significant main effect of training, $\beta = -4.05$, $z = -5.9$, $p < .001$. Participants (patients and controls) made more errors before (15.69 ± 0.13%) than after training (7.87 ± 0.1%). No significant interaction between group and training was found, $\beta = -1.06$, $z = -1.23$, $p = .22$, indicating that both groups improved their performance. However, a significant interaction between spatial frequency and training was observed, $\beta = -2.63$, $z = -3.1$, $p = .002$. Post-hoc comparisons showed that, across both groups, training significantly improved categorization for both LSF scenes (Before: 9.46 ± 0.14%; After: 4.33 ± 0.1%), $\beta = 4.63$, $z = 5.83$, $p < .001$, and HSF scenes (Before: 19.27 ± 0.15%; After: 10.67 ± 0.15%), $\beta = 2.01$, $z = 2.81$, $p = .005$. Although raw means suggested stronger improvement for HSF, the model-adjusted estimates revealed a larger effect for LSF ($\beta = 4.63$ vs. 2.01), reflecting the true effect once interindividual and item-level variance was accounted for.

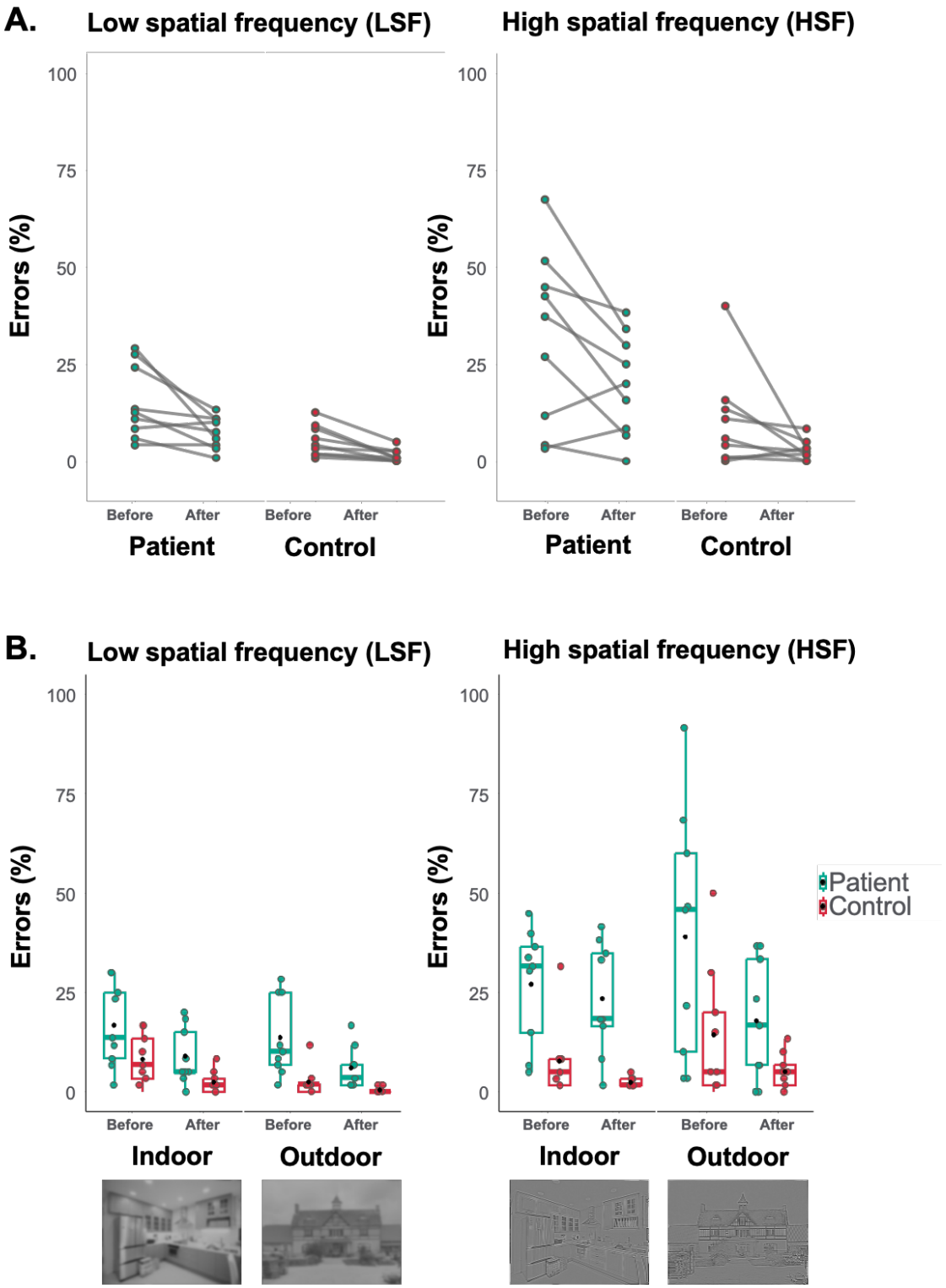

Figure 4. Error rates (%) in scene categorization with spatial frequency filtering for 9 patients and their 9 matched controls. (a) Data collapsed across scene category. For LSF and HSF, dots represent each participant's performance before and after training. Gray lines connect the two time points for the same participant. The left panel shows patients, and the right panel shows controls. (b) Data separated by scene category (indoor vs. outdoor). Boxplots indicate the median and quartiles, dots show each participant's mean performance. Black dots represent overall means, and error bars show the standard error of the mean.

A significant three-way interaction between group, spatial frequency, and training was also found, $\beta = -0.65$, $z = -3.73$, $p < .001$. Post-hoc comparisons showed that the group × training interaction was significant for LSF, $\beta = -1.21$, $z = -2.23$, $p = .03$ (HSF: $\beta = 0.22$, $z = 0.19$, $p = .85$): training significantly improved patients' performance for LSF scenes, $\beta = -2.6$, $z = -2.97$, $p = .006$, but not that of controls, $\beta = -1.13$, $z = -1.55$, $p = .24$. Patients made significantly fewer errors for LSF scenes after training (7.41 ± 0.19%) than before (15.11 ± 0.26%), whereas control participants were already accurate before training (Before: 5.28 ± 0.16%; After: 1.39 ± 0.08%). This suggests that the overall LSF improvement was mainly driven by patients. For HSF scenes, the group × training interaction was not significant, $\beta = 0.22$, $z = 0.19$, $p = .85$, indicating comparable improvements in both groups. Performance improved for HSF scenes in both patients (Before: 32.22 ± 0.34%; After: 19.81 ± 0.29%) and controls (Before: 10.19 ± 0.21%; After: 2.87 ± 0.12%), although improvement in patients remained partial due to residual high error rates, while control performance reached ceiling levels. Therefore, the global training effect was weaker for HSF than for LSF scenes.

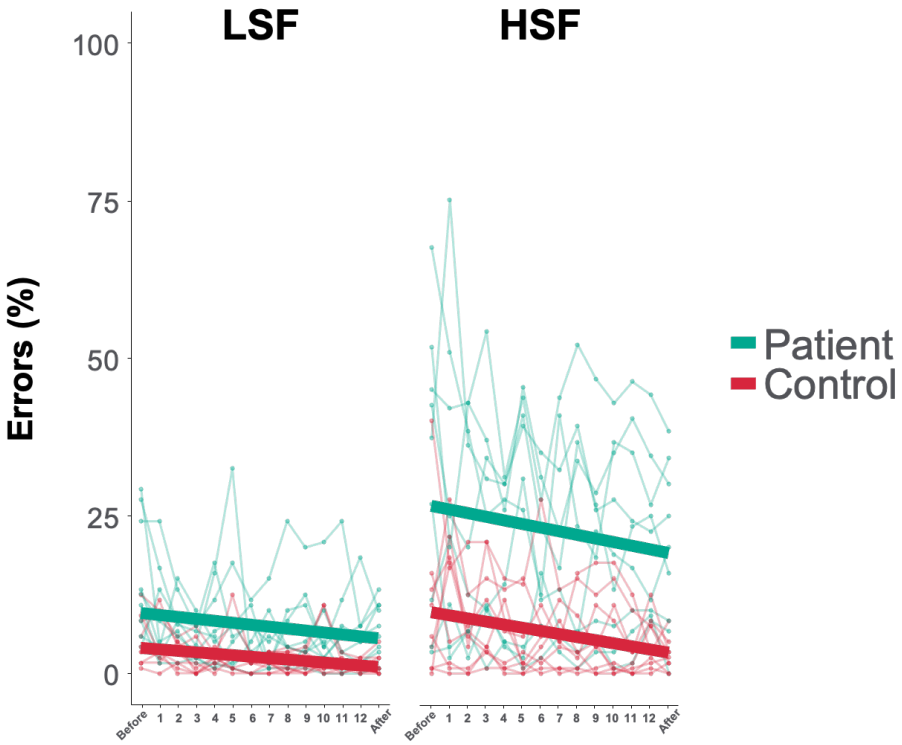

Figure 5. Evolution of average error rates across training sessions in MD patients (green) and matched controls (red), for scenes filtered in low spatial frequencies (LSF) and high spatial frequencies (HSF). Each line represents an individual participant; bold lines show average linear regressions for each condition. The x-axis represents training sessions 1–12 and the two evaluation sessions (before and after training).

A significant four-way interaction between group, training, spatial frequency, and semantic category was also observed, β = -5.67, z = -2.55, p = .01. Post-hoc comparisons showed that the interaction between spatial frequency, training, and category was only significant in patients, β = 4.43, z = 2.17, p = .03 (controls: β = -2.33, z = -0.45, p = .66). In patients, training improved performance for LSF scenes across both indoor and outdoor categories (see Figure 4b), whereas for HSF scenes the effect was selective. For patients, a significant training effect was observed only for HSF outdoor scenes, with a halving of error rates (Before: 38.96 ± 0.5%; After: 17.78 ± 0.39%), β = -4.08, z = -3.71, p < .001. HSF indoor scenes showed a smaller, non-significant change, β = -1.36, z = -1.45, p = .15 (Before: 25.46 ± 0.44%; After: 21.85 ± 0.42%).

We also tested the effect of training on categorization performance depending on the spatial frequency cut-offs (Figure 6). For LSF, the main effect of spatial frequency cut-off was not significant, β = -2.17, z = -1.81, p = .07. However, we observed a significant interaction effect between group, spatial frequency cut-off, and training, β = -2.69, z = -2.25, p = .03. When tested separately, the two-way interaction between spatial frequency cut-off and training was not significant in patients (β = 1.26, z = 0.79, p = .43) nor in controls (β = –0.32, z = –0.15, p = .88). The interaction between group and training reached significance only at 2 cpd, β = -2.6, z = -0.71, p = .03 (1 cpd: β = -0.69, z = -0.87, p = .39; 1.4 cpd: β = -1.44, z = -1.49, p = .14), suggesting that patients and controls did not respond in exactly the same way to training at this spatial frequency cutoff. However, post-hoc comparisons indicated that the training effect was not significant in either group, for patients (Before: 12.26 ± 0.41%; After: 7.5 ± 0.33%, β = –0.81, z = –0.71, p = .48) or for controls (Before: 3.61 ± 0.23%; After: 0.83 ± 0.11%, β = –2.38, z = –0.83, p = .40), indicating that the significant interaction should be interpreted with caution. The spatial frequency cut-off did not interact with the group, β = -1.27, z = -1.46, p = .15, nor training, β = 1.59, z = 0.79, p = .43, or scene category, β = -2.03, z = -1.31, p = .19, and the four variables did not interact, β = -1.7, z = -0.64, p = .53.

For HSF, analysis revealed a main effect of spatial frequency cut-off, β = -2.69, z = -2.34, p = .02. Post-hoc comparisons showed that participants made more errors at 6 cpd (21.47 ± 0.26%) than at both 4.6 cpd (15.99 ± 0.23%), β = -1.58, z = -2.16, p = .03, and 2.9 cpd (11.33 ± 0.2%), β = -1.71, z = -2.03, p = .02. However, the difference between 4.6 and 2.9 cpd was not significant, β = 0.26, z = 0.32, p = .75. The spatial frequency cut-off did not interact with any other variables (spatial frequency cut-off*group: β = -0.24, z = -0.14, p = .89; spatial frequency cut-off*training: β = -3.03, z = -1.66, p = .10; spatial frequency cut-off*training*group: β = -0.98, z = -0.31, p = .76; spatial frequency cut-

off*training*group*scene category: β = 0.88, z = 0.16, p = .87), suggesting that the decline in performance with increasing cutoff was comparable across groups, training conditions and scene categories.

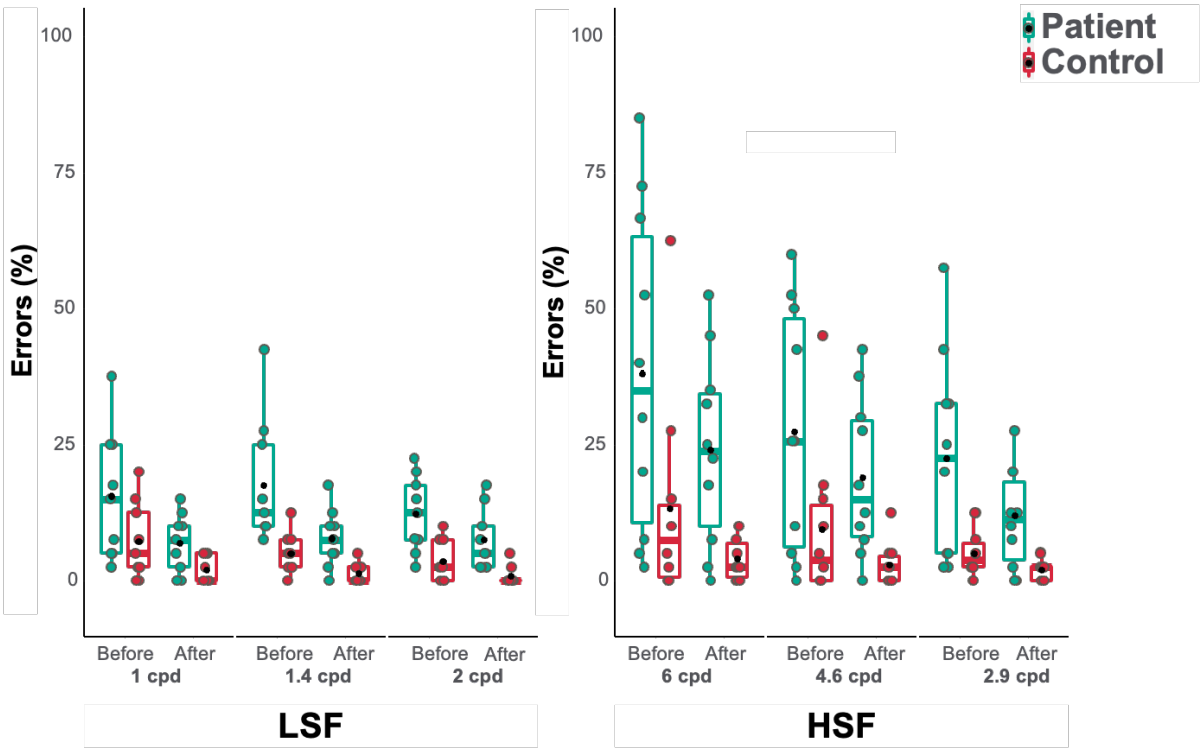

Figure 6. Error rates (%) for 9 patients and their matched control participants when categorizing low spatial frequency (LSF) and high spatial frequency (HSF) scenes at the different spatial frequency cutoffs, before and after training. Black dots indicate the overall mean and error bars show the standard error. Boxplots represent the median and quartiles, and individual dots represent each participant's average performance.

3.2.2. Visual acuity (FrACT), visual quality of life (NEI-VFQ 25), and mental health (BDI-II)

In the 9 patients included in the training analyses, the Wilcoxon paired-sample test revealed no significant difference in visual acuity (logMAR) before vs. after training, V = 23, p = .55. Although average BDI-II scores decreased after training (6.56 ± 2.03 vs. 4.68 ± 1.56), the difference was not statistically significant, V = 15, p = .054. Regarding quality of life, a significant improvement was observed on the "dependency" dimension of the NEI-VFQ 25 (After: 63.33 ± 8.89 vs. Before: 55.83 ± 7.76), V = 2.5, p = .05. No significant changes were found for the overall NEI-VFQ 25 score, V = 7, p = .07, nor for other dimensions.

4. Discussion

4.1. Impaired spatial frequency processing in elderly patients with MD

The behavioral results obtained before training confirm that patients with MD exhibit impaired scene categorization, particularly for HSF stimuli. When restricting the analysis to the nine patients over 50 years old and their matched controls, we found a significant interaction between group and spatial frequency: patients made significantly more errors for HSF scenes than for LSF scenes, and also significantly more errors than controls, but only for HSF stimuli. In contrast, no significant group difference was found for LSF scenes. These findings are consistent with previous work showing that central vision loss in MD primarily affects the processing of fine visual details carried by HSF, while LSF-based recognition is relatively preserved (Musel et al., 2011; Peyrin et al., 2017; Ramanoël et al., 2018). This dissociation is expected given the way central vision loss alters access to spatial frequency information. When central inputs are unavailable, visual processing shifts toward more eccentric retinal regions dominated by magnocellular pathways, which primarily transmit LSF information. As a result, LSF-based recognition remains relatively accessible through peripheral vision, whereas HSF processing is strongly degraded. This mechanism provides a straightforward explanation for why our patients showed preserved LSF performance relative to controls. This mechanism also suggests why training based on coarse visual information may help patients make better use of their remaining peripheral vision. Although this difference did not reach statistical significance, patients also tended to perform worse than controls for LSF scenes. This suggests that peripheral vision, although still functional, does not fully compensate for central vision loss.

To further examine this dissociation, we analyzed performance as a function of the specific spatial frequency cutoffs used to generate the filtered images. For LSF scenes, there was a significant main effect of cutoff: performance was worse at 1 cpd than at 2 cpd. The intermediate cutoff at 1.4 cpd did not significantly differ from either 1 or 2 cpd, suggesting a gradual improvement in performance as more spatial detail becomes available. The lack of interaction between group and cutoff indicates that this pattern was similar in both MD patients and controls. This pattern is consistent with the view that global visual information carried by LSF is relatively preserved in MD, although extremely coarse inputs remain challenging to interpret. For HSF scenes, performance declined as cutoff frequency increased, and this effect was significantly more pronounced in MD patients, who performed worse than controls at all cutoffs. The between-group difference grew larger at higher cutoffs, reaching nearly 27% at 6 cpd, consistent with a strong limitation in fine-detail processing through peripheral vision.

Controls also showed reduced accuracy at higher cutoffs, though to a lesser extent, suggesting that peripheral HSF processing is challenging even in healthy aging. These findings reinforce the idea that not all spatial frequency content is equally accessible in peripheral vision and highlight the compounded effects of aging and central vision loss on fine-detail processing.

Because one patient with Stargardt disease (MD10) was much younger than the rest of the MD group (25 years vs. 50–81 years) and showed very low error rates, we also ran a sensitivity analysis excluding this participant and the matched control. In the full sample, we observed significant main effects of group and spatial frequency, indicating overall poorer performance in MD than in controls and greater difficulty for HSF than for LSF scenes in both groups. In the reduced sample, the same pattern of main effects was observed and, in addition, the interaction between group and spatial frequency reached significance, revealing that the HSF deficit in MD was more pronounced than the LSF deficit when the influence of this atypical data point was removed. Given our small sample size and limited age range, this analysis was used solely as a robustness check. It cannot be interpreted as evidence regarding potential age effects on scene categorization.

Age-matched controls, although free of retinal pathology, also showed reduced performance for HSF scenes compared to LSF scenes when central vision was occluded. This finding is consistent with previous studies reporting age-related declines in fine-detail processing, likely due to decreased visual acuity and contrast sensitivity for HSF in normal aging (Elliott et al., 1995; Gittings & Fozard, 1986; Ramanoël et al., 2015). The HSF impairment observed in controls may therefore reflect the combined effects of age-related visual changes and the experimental constraint of peripheral viewing. Including a control group tested under equivalent visual constraints allowed us to determine that part of the performance decline for HSF scenes is not specific to MD, but may also result from normative aging when only peripheral inputs are available. This observation strengthens the rationale for perceptual training protocols targeting spatial frequency processing in peripheral vision, not only for rehabilitation in MD but also for supporting visuocognitive function in healthy aging.

4.2. Training effects on spatial frequency processing

Based on this rationale, we implemented a four-week visual training protocol consisting of twelve sessions in patients with MD. The aim was to help compensate for difficulties specifically related to HSF processing, and to enhance the use of both LSF and peripheral vision for scene recognition. To assess the potential generalizability of the protocol, we also included a group of age-matched control participants tested under equivalent peripheral

viewing conditions using artificial scotomas. These participants, although free of retinal pathology, also showed reduced HSF performance compared to LSF when relying solely on peripheral vision. This parallel suggests that such training programs could benefit not only clinical populations with central vision loss, but also older adults experiencing normative visual decline.

We observed a significant improvement in scene categorization performance for LSF stimuli in patients with MD, whereas no such improvement was observed in age-matched controls, whose performance for LSF scenes was already near ceiling before training. This suggests that the training enhanced patients' ability to use global visual cues in peripheral vision by strengthening LSF processing. When analyzing LSF cut-offs separately, statistical models indicated a group × training effect at 2 cpd. However, this effect was not corroborated by post-hoc comparisons within each group, which revealed no significant improvement after training. This pattern should therefore be interpreted with caution, as it likely reflects statistical noise rather than a robust training effect.

In contrast, both groups improved for HSF scenes, although patients' improvement remained partial due to initially high error rates. These training effects did not differ across HSF cutoffs, indicating that the improvements were consistent across the tested high-frequency ranges. Interestingly, the improvement in patients was selective to HSF outdoor scenes, which had elicited the greatest difficulties before training. This may seem counterintuitive, given that indoor scenes typically contain more HSF detail, which corresponds precisely to the type of information that patients with MD struggle to process in peripheral vision. However, the higher overall density of HSF content in indoor scenes may increase the chances that some diagnostic features are still accessible, even under degraded vision. In contrast, outdoor scenes often contain fewer and more spatially dispersed HSF cues, which may become entirely inaccessible when central vision is lost, making recognition particularly difficult before training but more responsive to improvement once compensatory mechanisms are reinforced.

We also observed a modest improvement in vision-related quality of life following training, particularly in the "dependency" subscale. This suggests that perceptual gains may have some functional relevance in daily life, even in the absence of measurable changes in visual acuity. Part of this benefit may also reflect motivational or relational aspects of the intervention, such as frequent contact with the experimenter and the feeling of being supported. While such factors are not specific to perceptual mechanisms, they likely contribute to the success and acceptability of training programs in older adults.

These preliminary results should be interpreted with caution. The small sample size limits the generalizability of the findings. Because intensive behavioral training requires strong patient commitment over several weeks, recruiting sufficiently large cohorts defined by disease type remains challenging. In the present sample, the small number of patients with Stargardt disease prevented formal statistical comparisons between etiologies. Future work with larger cohorts defined by disease type and with cone and rod mediated functional assessments will be necessary to determine whether training efficacy depends on disease etiology. Although the observed behavioral improvements are encouraging, future studies are needed to better understand the underlying mechanisms. In particular, combining this type of training with functional neuroimaging could elucidate how the brain adapts to visual training in peripheral vision, and clarify which neurocognitive mechanisms contribute to improved processing of spatial frequency information under peripheral viewing conditions. A likely hypothesis is that these behavioral improvements rely on plastic changes and functional reorganization within cortical regions that process input from the peripheral visual field. Recent findings indicate that MD alters spatial frequency processing even within the residual visual field, with marked deficits for HSF and relatively preserved processing of LSF. Functional MRI studies have also shown that HSF deficits are accompanied by reduced activation in occipital and category-selective regions, whereas LSF processing engages more distributed cortical networks, including frontoparietal and oculomotor areas involved in compensatory mechanisms. In this context, the improvement in LSF scene categorization observed after training may reflect an enhanced recruitment of these preserved pathways and a more efficient use of predictive and attentional resources. Moreover, previous studies have shown that striate areas can undergo retinotopic reorganization following central vision loss, with increased responsiveness to stimuli presented near the PRL (Baker et al., 2005; Dilks et al., 2009). This cortical adaptation may further support the shift toward global visual analysis based on LSF, which remains accessible in peripheral vision.

An additional mechanism that may contribute to the observed training effects is improved fixation stability at the PRL. Because the training protocol required repeated eccentric fixation on a central target, patients may have developed more stable fixation patterns over sessions. Increased fixation stability could ensure that HSF information is sampled with greater reliability by the same peripheral retinal region across trials. This may improve the overall accessibility of fine scene details, even though their spatial location varies from one image to another. Consistent with this possibility, previous work has shown that oculomotor training can improve fixation stability in patients with macular disease, with measurable

benefits for reading performance (Rosengarth et al., 2013). Although compatible with our behavioral findings, this mechanism remains speculative here because fixation stability was not directly monitored during training. This limitation motivates future studies combining scene-based perceptual training with eye-tracking and potentially pupillometry, in order to quantify whether changes in fixation stability or other oculomotor factors contribute to behavioral improvements.

Such functional adaptations are not exclusive to pathological conditions. Even in healthy vision, peripheral regions of the visual field are more sensitive to LSF, while HSF are preferentially processed through central vision (Henriksson et al., 2008; Musel et al., 2013). This intrinsic retinotopic organization supports the notion that peripheral vision is particularly suited for the extraction of coarse visual information. In contexts where central input is unavailable or suppressed, whether due to disease or experimental constraints as in the current study, such coarse cues become essential for recognition. Within predictive coding frameworks, early LSF information available in peripheral vision can initiate top-down expectations about scene content, thereby facilitating perceptual inference by constraining the interpretation of subsequent input (Peyrin et al., 2021). Our findings suggest that visual training may enhance these mechanisms, allowing both MD patients and older adults with simulated central loss to rely more effectively on coarse-level analysis and predictive guidance in peripheral vision.

Future studies should also assess whether these perceptual improvements generalize to other visual tasks, such as object detection, navigation, or face recognition, as well as to real-life situations. Longitudinal designs will be necessary to determine the stability of training effects over time and whether maintenance sessions are needed. In addition, the absence of a sham or placebo training condition prevents us from fully disentangling task-specific learning effects from non-specific influences such as repeated testing, procedural familiarity, motivation, or experimenter contact. Future studies could implement such a control condition, for example by training with stimuli with uninformative spatial-frequency content, while matching all other aspects of the procedure. Finally, the demonstration of training-related improvements suggests that this protocol may provide a useful basis for rehabilitation. Building on this result, future clinical applications could combine the training with contrast sensitivity function (CSF) assessments to adapt stimulation to each patient's visual profile, since CSF profiles indicate how sensitivity varies across spatial frequencies. This information could be used pragmatically to adjust stimulus contrast and spatial-frequency parameters to individual residual sensitivity when implementing personalized rehabilitation in routine care.

5. Conclusion

This study provides novel behavioral evidence that spatial frequency training can enhance scene categorization in peripheral vision, particularly in patients with MD. Improvements were most notable for LSF scenes and, to a lesser extent, for outdoor HSF scenes, which initially posed the greatest difficulty. These findings support the potential of perceptual learning protocols to compensate for central vision loss by reinforcing the use of residual peripheral vision. Beyond clinical applications, the observation that older adults without MD also show deficits in HSF processing under peripheral viewing conditions highlights a broader phenomenon associated with normal aging. Targeted visual training may thus benefit not only patients with MD but also healthy older individuals, by supporting peripheral processing and compensatory strategies. In the long term, such interventions could help preserve functional autonomy by reinforcing visuocognitive abilities essential to daily life.

Acknowledgments: This work was supported by a French grant from the Agence Nationale de la Recherche (ANR-21-CE28-0021).

References

Allikmets, R., Shroyer, N. F., Singh, N., Seddon, J. M., Lewis, R. A., Bernstein, P. S., Peiffer, A., Zabriskie, N. A., Li, Y., Hutchinson, A., Dean, M., Lupski, J. R., & Leppert, M. (1997). Mutation of the Stargardt disease gene (ABCR) in age-related macular degeneration. Science (New York, N.Y.), 277(5333), 1805–1807. https://doi.org/10.1126/science.277.5333.1805

Awan, M. A., & Tarin, S. A. (2006). Review of photodynamic therapy. The surgeon : journal of the Royal Colleges of Surgeons of Edinburgh and Ireland, 4(4), 231–236. https://doi.org/10.1016/s1479-666x(06)80065-x

Bach M. (2007). The Freiburg Visual Acuity Test-variability unchanged by post-hoc re-analysis. Graefe's archive for clinical and experimental ophthalmology = Albrecht von Graefes Archiv fur klinische und experimentelle Ophthalmologie, 245(7), 965–971. https://doi.org/10.1007/s00417-006-0474-4

Baker, C. I., Peli, E., Knouf, N., Kanwisher, N. G., 2005. Reorganization of visual processing in macular degeneration. The Journal of neuroscience : the official journal of the Society for Neuroscience 25 (3), 614–618. https://doi.org/10.1523/JNEUROSCI.3476-04.2005.

Barboni, M. T. S., Récsán, Z., Szepessy, Z., Ecsedy, M., Nagy, B. V., Ventura, D. F., Nagy, Z. Z., & Németh, J. (2019). Preliminary Findings on the Optimization of Visual Performance in Patients with Age-Related Macular Degeneration Using Biofeedback Training. Applied psychophysiology and biofeedback, 44(1), 61–70. https://doi.org/10.1007/s10484-018-9423-3

Bates, D., Kliegl, R., Vasishth, S., & Baayen, H. (2015). Parsimonious mixed models. arXiv preprint arXiv:1506.04967.

Bates, D., Mächler, M., Bolker, B., & Walker, S. (2015). Fitting linear mixed-effects models using lme4. Journal of statistical software, 67, 1-48. https://doi/org/10.18637/jss.v067.i01

Beck, A. T., Steer, R. A., & Brown, G. K. (1996). Beck depression inventory.

Boucart, M., Despretz, P., Hladiuk, K., & Desmettre, T. (2008a). Does context or color improve object recognition in patients with low vision?. Visual neuroscience, 25(5-6), 685–691. https://doi.org/10.1017/S0952523808080826

Boucart, M., Dinon, J. F., Despretz, P., Desmettre, T., Hladiuk, K., & Oliva, A. (2008b). Recognition of facial emotion in low vision: a flexible usage of facial features. Visual neuroscience, 25(4), 603–609. https://doi.org/10.1017/S0952523808080656

Brainard, D. H. (1997). The psychophysics toolbox. Spatial vision, 10(4), 433-436.

Brody, B. L., Gamst, A. C., Williams, R. A., Smith, A. R., Lau, P. W., Dolnak, D., Rapaport, M. H., Kaplan, R. M., & Brown, S. I. (2001). Depression, visual acuity, comorbidity, and disability associated with age-related macular degeneration. Ophthalmology, 108(10), 1893–1901. https://doi.org/10.1016/s0161-6420(01)00754-0

Brown, M. M., Brown, G. C., Sharma, S., Landy, J., & Bakal, J. (2002). Quality of life with visual acuity loss from diabetic retinopathy and age-related macular degeneration. Archives of ophthalmology, 120(4), 481-484. https://doi.org/10.1001/archopht.120.4.481

Bullimore, M. A., Bailey, I. L., & Wacker, R. T. (1991). Face recognition in age-related maculopathy. Investigative ophthalmology & visual science, 32(7), 2020-2029.

Calabrèse, A., Bernard, J. B., Hoffart, L., Faure, G., Barouch, F., Conrath, J., & Castet, E. (2011). Wet versus dry age-related macular degeneration in patients with central field loss: different effects on maximum reading speed. Investigative ophthalmology & visual science, 52(5), 2417–2424. https://doi.org/10.1167/iovs.09-5056

Casco, C., Campana, G., Grieco, A., & Fuggetta, G. (2004). Perceptual learning modulates electrophysiological and psychophysical response to visual texture segmentation in

humans. Neuroscience letters, 371(1), 18–23. https://doi.org/10.1016/j.neulet.2004.08.005

Chung S. T. (2011). Improving reading speed for people with central vision loss through perceptual learning. Investigative ophthalmology & visual science, 52(2), 1164–1170. https://doi.org/10.1167/iovs.10-6034

Crossland, M. D., Crabb, D. P., & Rubin, G. S. (2011). Task-specific fixation behavior in macular disease. Investigative ophthalmology & visual science, 52(1), 411–416. https://doi.org/10.1167/iovs.10-5473

Culham, L. E., Fitzke, F. W., & Marshall, J. (1997). Training of patients with age-related macular disease (AMD) using a scanner laser ophthalmoscope (SLO). Ophthalmic and Physiological Optics, 17(6), 542-542. https://doi.org/10.1016/j.ophtha.2006.06.028

Curcio, C. A., & Allen, K. A. (1990). Topography of ganglion cells in human retina. The Journal of comparative neurology, 300(1), 5–25. https://doi.org/10.1002/cne.903000103

Curcio, C. A., Sloan, K. R., Kalina, R. E., & Hendrickson, A. E. (1990). Human photoreceptor topography. The Journal of comparative neurology, 292(4), 497–523. https://doi.org/10.1002/cne.902920402

Dilks, D. D., Baker, C. I., Peli, E., Kanwisher, N., 2009. Reorganization of visual processing in macular degeneration is not specific to the "preferred retinal locus. The Journal of neuroscience : the official journal of the Society for Neuroscience 29 (9), 2768–2773. https://doi.org/10.1523/JNEUROSCI.5258-08.2009.

Elliott, D. B., Yang, K. C., & Whitaker, D. (1995). Visual acuity changes throughout adulthood in normal, healthy eyes: seeing beyond 6/6. Optometry and vision science: official publication of the American Academy of Optometry, 72(3), 186–191. https://doi.org/10.1097/00006324-199503000-00006

Faurite, C., Michaud, C., Cousin, E., Olivier, P., Gallice, M., Chiquet, C., Pietras, J., Attyé, A., Soler, V., Berry, I., Mermillod, M., Cottereau, B. R., & Peyrin, C. (2025). Neurobehavioral Changes in Macular Degeneration: Spatial Frequency Use in Scene Recognition. Investigative ophthalmology & visual science, 66(13), 54. https://doi.org/10.1167/iovs.66.13.54

Fine, E. M., Peli, E., & Labianca, A. T. (1995, February). Reading of Dynamically Displayed Text by Low Vision Observers. In Vision Science and its Applications (p. SuB4). Optica Publishing Group. https://doi.org/10.1364/VSIA.1995.SuB4

Fletcher, D. C., Schuchard, R. A., & Watson, G. (1999). Relative locations of macular scotomas near the PRL: effect on low vision reading. Journal of rehabilitation research and development, 36(4), 356–364.

GBD 2021 Global AMD Collaborators (2025). Global burden of vision impairment due to age-related macular degeneration, 1990-2021, with forecasts to 2050: a systematic analysis for the Global Burden of Disease Study 2021. The Lancet. Global health, 13(7), e1175–e1190. https://doi.org/10.1016/S2214-109X(25)00143-3

Gittings, N. S., & Fozard, J. L. (1986). Age related changes in visual acuity. Experimental gerontology, 21(4-5), 423–433. https://doi.org/10.1016/0531-5565(86)90047-1

Guénot, J., Trotter, Y., Fricker, P., Cherubini, M., Soler, V., & Cottereau, B. R. (2022). Optic flow processing in patients with macular degeneration. Investigative Ophthalmology & Visual Science, 63(12), 21-21.

Hassan, S. E., Lovie-Kitchin, J. E., & Woods, R. L. (2002). Vision and mobility performance of subjects with age-related macular degeneration. Optometry and vision science, 79(11), 697-707.

Henriksson, L., Nurminen, L., Hyvärinen, A., & Vanni, S. (2008). Spatial frequency tuning in human retinotopic visual areas. Journal of vision, 8(10), 1–13. https://doi.org/10.1167/8.10.5

Hussain, R. M., & Ciulla, T. A. (2017). Emerging vascular endothelial growth factor antagonists to treat neovascular age-related macular degeneration. Expert opinion on emerging drugs, 22(3), 235–246. https://doi.org/10.1080/14728214.2017.1362390

Karni, A., & Sagi, D. (1991). Where practice makes perfect in texture discrimination: evidence for primary visual cortex plasticity. Proceedings of the National Academy of Sciences of the United States of America, 88(11), 4966–4970. https://doi.org/10.1073/pnas.88.11.4966

Kleiner, M., Brainard, D., Pelli, D., Ingling, A., Murray, R., & Broussard, C. (2007). What's new in psychtoolbox-3. Perception, 36(14), 1–16.

Legge, G. E., Ross, J. A., Isenberg, L. M., & Lamay, J. M. (1992). Psychophysics of reading. Clinical predictors of low-vision reading speed. Investigative Ophthalmology & Visual Science, 33(3), 677-687.

Lim, L. S., Mitchell, P., Seddon, J. M., Holz, F. G., & Wong, T. Y. (2012). Age-related macular degeneration. Lancet (London, England), 379(9827), 1728–1738. https://doi.org/10.1016/S0140-6736(12)60282-7

Logan, A. J., Gordon, G. E., & Loffler, G. (2020). The Effect of Age-Related Macular Degeneration on Components of Face Perception. Investigative ophthalmology & visual science, 61(6), 38. https://doi.org/10.1167/iovs.61.6.38

Mangione, C. M., Lee, P. P., Pitts, J., Gutierrez, P., Berry, S., & Hays, R. D. (1998). Psychometric properties of the National Eye Institute Visual Function Questionnaire (NEI-VFQ). NEI-VFQ Field Test Investigators. Archives of ophthalmology (Chicago, Ill.: 1960), 116(11), 1496–1504. https://doi.org/10.1001/archopht.116.11.1496

Maniglia, M., Pavan, A., Cuturi, L. F., Campana, G., Sato, G., & Casco, C. (2011). Reducing crowding by weakening inhibitory lateral interactions in the periphery with perceptual learning. PloS one, 6(10), e25568. https://doi.org/10.1371/journal.pone.0025568

Maniglia, M., Pavan, A., Sato, G., Contemori, G., Montemurro, S., Battaglini, L., & Casco, C. (2016). Perceptual learning leads to long lasting visual improvement in patients with central vision loss. Restorative neurology and neuroscience, 34(5), 697–720. https://doi.org/10.3233/RNN-150575

Maniglia, M., Soler, V., Cottereau, B., & Trotter, Y. (2018). Spontaneous and training-induced cortical plasticity in MD patients: Hints from lateral masking. Scientific reports, 8(1), 90. https://doi.org/10.1038/s41598-017-18261-6

Melillo, P., Prinster, A., Di Iorio, V., Olivo, G., D'Alterio, F. M., Cocozza, S., Quarantelli, M., Testa, F., Brunetti, A., & Simonelli, F. (2020). Biofeedback Rehabilitation and Visual Cortex Response in Stargardt's Disease: A Randomized Controlled Trial. Translational vision science & technology, 9(6), 6. https://doi.org/10.1167/tvst.9.6.6

Michaud, C., Guénot, J., Faurite, C., Gallice, M., Chiquet, C., Vayssière, N., Berry, I., Trotter, Y., Soler, V., Peyrin, C., & Cottereau, B. R. (2025). Motion Processing in Visual Cortex of Maculopathy Patients. The Journal of neuroscience: the official journal of the Society for Neuroscience, 45(30), e0283252025. https://doi.org/10.1523/JNEUROSCI.0283-25.2025

Mitchell, J., & Bradley, C. (2006). Quality of life in age-related macular degeneration: a review of the literature. Health and quality of life outcomes, 4(1), 97. https://doi.org/10.1186/1477-7525-4-97

Musel, B., Bordier, C., Dojat, M., Pichat, C., Chokron, S., Le Bas, J. F., & Peyrin, C. (2013). Retinotopic and lateralized processing of spatial frequencies in human visual cortex during scene categorization. Journal of cognitive neuroscience, 25(8), 1315–1331. https://doi.org/10.1162/jocn_a_00397

Musel, B., Hera, R., Chokron, S., Alleysson, D., Chiquet, C., Romanet, J. P., Guyader, N., & Peyrin, C. (2011). Residual abilities in age-related macular degeneration to process spatial frequencies during natural scene categorization. Visual neuroscience, 28(6), 529–541. https://doi.org/10.1017/S0952523811000435

Peli, E., Lee, E., Trempe, C. L., & Buzney, S. (1994). Image enhancement for the visually impaired: the effects of enhancement on face recognition. Journal of the Optical Society of America A, 11(7), 1929-1939. https://doi.org/10.1364/JOSAA.11.001929

Peyrin, C., Ramanoël, S., Roux-Sibilon, A., Chokron, S., & Hera, R. (2017). Scene perception in age-related macular degeneration: Effect of spatial frequencies and contrast in residual vision. Vision research, 130, 36–47. https://doi.org/10.1016/j.visres.2016.11.004

Peyrin, C., Roux-Sibilon, A., Trouilloud, A., Khazaz, S., Joly, M., Pichat, C., Boucart, M., Krainik, A., & Kauffmann, L. (2021). Semantic and Physical Properties of Peripheral Vision Are Used for Scene Categorization in Central Vision. Journal of cognitive neuroscience, 33(5), 799–813. https://doi.org/10.1162/jocn_a_01689

Ramanoël, S., Chokron, S., Hera, R., Kauffmann, L., Chiquet, C., Krainik, A., & Peyrin, C. (2018). Age-related macular degeneration changes the processing of visual scenes in the brain. Visual neuroscience, 35, E006. https://doi.org/10.1017/S0952523817000372

Ramanoël, S., Kauffmann, L., Cousin, E., Dojat, M., & Peyrin, C. (2015). Age-Related Differences in Spatial Frequency Processing during Scene Categorization. PloS one, 10(8), e0134554. https://doi.org/10.1371/journal.pone.0134554

Rosengarth, K., Keck, I., Brandl-Rühle, S., Frolo, J., Hufendiek, K., Greenlee, M. W., & Plank, T. (2013). Functional and structural brain modifications induced by oculomotor training in patients with age-related macular degeneration. Frontiers in psychology, 4, 428. https://doi.org/10.3389/fpsyg.2013.00428

Rovner, B. W., & Casten, R. J. (2002). Activity loss and depression in age-related macular degeneration. The American journal of geriatric psychiatry, 10(3), 305-310. https://doi.org/10.1097/00019442-200205000-00010

Sahli, E., Altinbay, D., Bingol Kiziltunc, P., & Idil, A. (2020). Effectiveness of Low Vision Rehabilitation Using Microperimetric Acoustic Biofeedback Training in Patients with Central Scotoma. Current eye research, 46(5), 731–738. https://doi.org/10.1080/02713683.2020.1833348

Salive, M. E., Guralnik, J., Glynn, R. J., Christen, W., Wallace, R. B., & Ostfeld, A. M. (1994). Association of visual impairment with mobility and physical function. Journal of the

American Geriatrics Society, 42(3), 287-292. https://doi.org/10.1111/j.1532-5415.1994.tb01753.x

Sasso, P., Silvestri, V., Sulfaro, M., Scupola, A., Fasciani, R., & Amore, F. (2019). Perceptual learning in patients with Stargardt disease. Canadian journal of ophthalmology. Journal canadien d'ophtalmologie, 54(6), 708–716. https://doi.org/10.1016/j.jcjo.2019.03.012

Seiple, W., Szlyk, J. P., McMahon, T., Pulido, J., & Fishman, G. A. (2005). Eye-movement training for reading in patients with age-related macular degeneration. Investigative ophthalmology & visual science, 46(8), 2886–2896. https://doi.org/10.1167/iovs.04-1296

Shah, N. J., & Shah, U. N. (2011). Long-term effect of early intervention with single intravitreal injection of bevacizumab followed by panretinal and macular grid photocoagulation in central retinal vein occlusion (CRVO) with macular edema: a pilot study. Eye, 25(2), 239-244. https://doi.org/10.1038/eye.2010.225

Šimkovic, M., and Träuble, B. (2019). Robustness of statistical methods when measure is affected by ceiling and/or floor effect. PLOS ONE, 14(8), e0220889. https://doi.org/10.1371/journal.pone.0220889

Solomon, S. D., Lindsley, K., Vedula, S. S., Krzystolik, M. G., & Hawkins, B. S. (2019). Anti-vascular endothelial growth factor for neovascular age-related macular degeneration. The Cochrane database of systematic reviews, 3(3), CD005139. https://doi.org/10.1002/14651858.CD005139.pub4

Sunness, J. S., Applegate, C. A., Haselwood, D., & Rubin, G. S. (1996). Fixation patterns and reading rates in eyes with central scotomas from advanced atrophic age-related macular degeneration and Stargardt disease. Ophthalmology, 103(9), 1458–1466. https://doi.org/10.1016/s0161-6420(96)30483-1

Tarita-Nistor, L., Sverdlichenko, I., & Mandelcorn, M. S. (2023). What Is a Preferred Retinal Locus?. Annual review of vision science, 9, 201–220. https://doi.org/10.1146/annurev-vision-111022-123909

Tejeria, L., Harper, R. A., Artes, P. H., & Dickinson, C. M. (2002). Face recognition in age related macular degeneration: perceived disability, measured disability, and performance with a bioptic device. British Journal of Ophthalmology, 86(9), 1019-1026. https://doi.org/10.1136/bjo.86.9.1019

Thomas, C. J., Mirza, R. G., & Gill, M. K. (2021). Age-Related Macular Degeneration. The Medical Clinics of North America, 105(3), 473–491. https://doi.org/10.1016/j.mcna.2021.01.003

van Huet, R. A., Bax, N. M., Westeneng-Van Haaften, S. C., Muhamad, M., Zonneveld-Vrieling, M. N., Hoefsloot, L. H., Cremers, F. P., Boon, C. J., Klevering, B. J., & Hoyng, C. B. (2014). Foveal sparing in Stargardt disease. Investigative ophthalmology & visual science, 55(11), 7467–7478. https://doi.org/10.1167/iovs.13-13825

Wässle, H., Grünert, U., Röhrenbeck, J., & Boycott, B. B. (1990). Retinal ganglion cell density and cortical magnification factor in the primate. Vision research, 30(11), 1897–1911. https://doi.org/10.1016/0042-6989(90)90166-i

Wong, W. L., Su, X., Li, X., Cheung, C. M., Klein, R., Cheng, C. Y., & Wong, T. Y. (2014). Global prevalence of age-related macular degeneration and disease burden projection for 2020 and 2040: a systematic review and meta-analysis. The Lancet. Global health, 2(2), e106–e116. https://doi.org/10.1016/S2214-109X(13)70145-1

Zhang, S., Ren, J., Chai, R., Yuan, S., & Hao, Y. (2024). Global burden of low vision and blindness due to age-related macular degeneration from 1990 to 2021 and projections for 2050. BMC public health, 24(1), 3510. https://doi.org/10.1186/s12889-024-21047-x